Second-harmonic generation optical activity of a polypeptide α-helix at the air/water interface

S. A. Mitchell, R. A. McAloney, D. Moffatt, N. Mora-Diez,[a] and M. Z. Zgierski
Steacie Institute for Molecular Sciences, National Research Council of Canada, 100 Sussex Drive, Ottawa, Ontario K1A 0R6, Canada

(Received 25 October 2004; accepted 5 January 2005; published online 18 March 2005)

Quantitative measurements of second-harmonic generation optical activity (SHG-OA) have been performed for α-helical polypeptides poly-(γ-benzyl-*L*-glutamate) and poly-(γ-ethyl-*L*-glutamate) adsorbed at the air/water interface, with the fundamental frequency $\hbar\omega = 2.96$ eV ($\lambda = 417$ nm). The chiral component of the nonlinear susceptibility $\chi^{(2)}_{XYZ}$ is small for both polymers, being comparable in magnitude with the susceptibility $\chi^{(2)}_{XXZ}$ of the clean air/water interface. The microscopic origin of the nonlinear response has been investigated by using semiempirical ZINDO/S calculations in conjunction with standard time-dependent perturbation theory to evaluate the molecular hyperpolarizability tensor of a model α-helix composed of glycine residues. Calculated nonlinear susceptibilities (per monomer unit) are in good agreement with experimental measurements for both the chiral and achiral response. The computational results indicate that charge transfer transitions of the α-helix have a large influence on the achiral components of the hyperpolarizability tensor, and produce characteristic features in the response under suitable experimental conditions. The dominant origin of SHG-OA for the model α-helix is a structural effect due to the tilt of the plane of each amide group of the helix relative to the helical axis. SHG-OA is associated with the orientational distribution of isolated, achiral chromophores, and is present in the absence of electronic coupling between the amide subunits of the polypeptide α-helix. © *2005 American Institute of Physics*. [DOI: 10.1063/1.1862613]

I. INTRODUCTION

[1]Chirality is ubiquitous in biomolecules. Its manifestations in optical activity of biomolecules in linear optics are well known and include optical rotation and circular dichroism.[1] In contrast, chiral effects in nonlinear optics are relatively new, and there are only a few reports of *nonlinear* optical activity of biomolecules.[2,3] Second-harmonic generation optical activity (SHG-OA) has been observed for a variety of chiral interfaces and thin films,[2] and is well understood on a phenomenological level as a material response of a macroscopically chiral surface,[4] i.e., a surface that lacks mirror planes. SHG-OA is generally observed as a differential response in SHG for left- and right-hand circularly polarized fundamental light incident on the surface. Several reports have described SHG-OA of biomolecular interfaces.[2,5–7] However, the microscopic origin of SHG-OA is not well understood, and thus the potential of SHG-OA for probing the structure and organization of biomolecular interfaces is not known.

Recently, Conboy and Kriech[5,6] (CK) reported SHG-OA measurements for the peptide melittin adsorbed on a planar supported lipid bilayer. In the work of CK the fundamental radiation was in the wavelength region $\lambda = 410-470$ nm, such that the second-harmonic wavelength $\lambda/2$ was close to resonance with the amide transitions of the peptide backbone, ~220 nm. It is well known that this UV region shows characteristic features in circular dichroism spectroscopy which are diagnostic of the secondary structures of polypeptide chains.[8] CK suggested that the SHG-OA response of adsorbed melittin was associated with amide chromophores of an α-helical peptide backbone. However, each unit of melittin includes a tryptophan residue, so it is not clear whether the SHG-OA effects observed by CK were associated with the peptide backbone of melittin or with the aromatic side chain. The possibility of contributions from aromatic amino acids is shown by previous work from this laboratory in which a significant SHG-OA response was observed for simple tryptophan derivatives adsorbed at the air/water interface.[7]

In this work we have investigated the specific SHG-OA response of a polypeptide α-helix adsorbed at the air/water interface, with the fundamental wavelength $\lambda = 417$ nm. Two polypeptides, poly-(γ-benzyl-*L*-glutamate) (PBLG) **1** and poly-(γ-ethyl-*L*-glutamate) (PELG) **2**, were studied as Langmuir films spread on water:

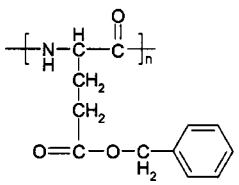

1

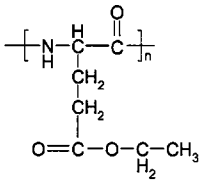

2

It is well established that these polymers adopt α-helical conformations at the air/water interface, with the long axis of the helix parallel to the interfacial plane.[9] Here we report the observation of a small SHG-OA response for PBLG and

[a]Present address: Department of Chemistry, Thompson Rivers University, Kamloops, British Columbia V2E 5N3, Canada.

PELG, which is associated with the α-helical conformation of the polypeptide chain. We also report the results of computations using a sum-over-states approach to calculate the molecular hyperpolarizability tensor of a model α-helix composed of glycine residues. The calculations provide insight into the microscopic origin of the chiral and achiral components of the SHG response of a polypeptide α-helix. In particular, we highlight the important role of the orientational distribution of the chromophoric subunits of the polypeptide molecular structure. It is shown that the SHG-OA response can be understood in a simple way as arising from a small tilt of the planes of the individual amide chromophores relative to the long axis of the helix. A similar structural origin for SHG-OA of chiral interfaces composed of achiral chromophores has been proposed by Simpson and co-workers.[10–12] In this work we present a detailed investigation of this effect for the particular case of a polypeptide α-helix.

II. EXPERIMENTAL SECTION

PBLG and PELG from Sigma-Aldrich were spread at the air/water interface from ~1 mg/ml solutions in HPLC grade chloroform (Fisher Scientific). The degree of polymerization quoted by the manufacturer was ~500 for PBLG and ~1700 for PELG (measured by viscosity). The surface pressure was monitored by using a NIMA model 102M Langmuir film balance fabricated from poly(tetrafluoroethylene) and equipped with a Wilhelmy plate surface pressure sensor. The Wilhelmy plate was a strip of chromatography paper. Milli-*Q* (18 MΩ cm) water was used as the subphase. All measurements were at room temperature, 22 °C.

Details of the laser source and experimental arrangement for SHG-OA measurements have been described previously.[7] Laser pulses with duration ~80 fs from a 1 kHz regenerative amplifier operating at 834 nm were frequency doubled to 417 nm in a BBO crystal. The intensity and polarization state of 417 nm radiation were controlled by using a Berek's polarization compensator followed by a Glan-laser calcite polarizer and a zero-order quarter-wave retardation plate. The laser beam was focused on the air/water interface with a 30 cm focal length lens, with the pulse energy ~5 μJ at 417 nm. The angle of incidence was 60°. Reflected second-harmonic radiation with $\lambda \sim 208$ nm was resolved in *p*- or *s*-polarization components by using a MgF_2 Rochon prism and detected on a solar-blind photomultiplier tube. A Pellin–Broca prism and a pair of dichroic mirrors were used to reject light at the fundamental frequency. The SHG signal from the air/water interface was normalized for intensity fluctuations of the fundamental by using a reference SHG signal from a quartz plate that was measured simultaneously with the sample signal.

III. COMPUTATIONAL METHOD

The ZINDO/S semiempirical method implemented in the Gaussian program package G98W (Ref. 13) was used to calculate the electronic structure of a model polypeptide α-helix composed of seven glycine residues. The parametrization of ZINDO/S was that of Ridley and Zerner[14] and Bacon and Zerner.[15] Excitation energies and electric dipole transition moments for 80 excited electronic states were derived from a CIS calculation including 30 occupied and 30 unoccupied molecular orbitals of the ground electronic state of the α-helix. Transition moments were calculated for transitions from the ground state to all excited states and for transitions between all excited states. Static molecular dipole moments of the ground and excited electronic states were calculated from density matrices for the electronic states available in the G98W checkpoint file.[16] Similar calculations were performed for the individual *N*-methylacetamide (NMA) subunits of the α-helix. For these calculations, 50 excited electronic states were derived from a CIS calculation including ten occupied and ten unoccupied molecular orbitals of the ground electronic state of the NMA monomer. This computational approach has been shown to give good results for the spectroscopic properties of simple amides, including excitation energies and transition dipole moments.[17,18] Our results for the ground and low lying excited states of NMA compare favorably with experimental measurements and *ab initio* calculations on NMA and related amides.[19,20]

The molecular hyperpolarizability tensor $\beta_{ijk}(\omega)$ was calculated by substituting the results of the ZINDO/S calculations in the appropriate sum-over-states expression[21] from standard time-dependent perturbation theory. The expression for SHG with all quantities expressed in atomic units is given in Eq. (1). The first and second terms in Eq. (1) are sums,

$$\begin{aligned}\beta_{ijk}(\omega) = \frac{1}{8}\sum_{n}\sum_{n'\neq n}\{&(\mu^{j}_{gn'}\mu^{i}_{n'n}\mu^{k}_{gn} + \mu^{k}_{gn'}\mu^{i}_{n'n}\mu^{j}_{gn})A \\ &+ (\mu^{i}_{gn'}\mu^{j}_{n'n}\mu^{k}_{gn} + \mu^{i}_{gn'}\mu^{k}_{n'n}\mu^{j}_{gn})B \\ &+ (\mu^{j}_{gn'}\mu^{k}_{n'n}\mu^{i}_{gn} + \mu^{k}_{gn'}\mu^{j}_{nn'n}\mu^{i}_{gn})C\} \\ &+ \frac{1}{4}\sum_{n}\{2\Delta\mu^{i}_{n}\mu^{j}_{gn}\mu^{k}_{gn}D + \mu^{i}_{gn}(\Delta\mu^{j}_{n}\mu^{k}_{gn} \\ &+ \Delta\mu^{k}_{n}\mu^{j}_{gn})E\},\end{aligned} \tag{1}$$

over all pairs of excited electronic states (n,n'), and over individual excited electronic states n, respectively. The ground electronic state is designated g. The quantities $\mu^{i}_{gn'}$ and $\mu^{i}_{nn'}$ are Cartesian components of electric dipole transition matrix elements, $\mu^{i}_{gn'} = -\langle g|r_i|n'\rangle$, and $\Delta\mu^{i}_{n} = (\mu^{i}_{nn} - \mu^{i}_{gg})$ is the difference in static molecular dipole moments between ground and excited electronic states. The quantities A, B, C, D, and E are given in Eqs. (2)–(6), where ε is the energy corresponding to the incident laser frequency and ε_{ng} is the excitation energy of state n. Damping was included in the calculations by

$$A = [(\varepsilon_{n'g} - \varepsilon)(\varepsilon^{*}_{ng} + \varepsilon)]^{-1} + [(\varepsilon^{*}_{n'g} + \varepsilon)(\varepsilon_{ng} - \varepsilon)]^{-1}, \tag{2}$$

$$B = [(\varepsilon^{*}_{n'g} + 2\varepsilon)(\varepsilon^{*}_{ng} + \varepsilon)]^{-1} + [(\varepsilon_{n'g} - 2\varepsilon)(\varepsilon_{ng} - \varepsilon)]^{-1}, \tag{3}$$

$$C = [(\varepsilon_{n'g} - \varepsilon)(\varepsilon_{ng} - 2\varepsilon)]^{-1} + [(\varepsilon^{*}_{n'g} + \varepsilon)(\varepsilon^{*}_{ng} + 2\varepsilon)]^{-1}, \tag{4}$$

$$D = [(\varepsilon_{ng} - \varepsilon)(\varepsilon^{*}_{ng} + \varepsilon)]^{-1}, \tag{5}$$

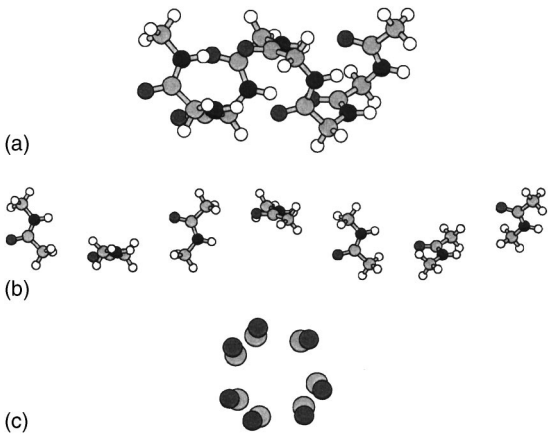

FIG. 1. Model right-handed α-helix composed of seven glycine residues. (a) Illustration of molecular structure showing carbon, oxygen, and nitrogen atoms in progressively darker shades of gray. Hydrogen atoms are shown in white. (b) Division of model α-helix into seven *N*-methylacetamide monomers, with the orientations of the amide groups preserved. (c) End-on view of model α-helix, showing only the carbonyl groups. Note that the CO bonds are tilted away from the long axis of the helix.

$$E = [(\varepsilon_{ng}^{*} + 2\varepsilon)(\varepsilon_{ng}^{*} + \varepsilon)]^{-1} + [(\varepsilon_{ng} - 2\varepsilon)(\varepsilon_{ng} - \varepsilon)]^{-1}, \quad (6)$$

using the substitutions $\varepsilon_{ng} \rightarrow \varepsilon_{ng} - i\Gamma$ and $\varepsilon_{ng}^{*} \rightarrow \varepsilon_{ng} + i\Gamma$,[21] with $\Gamma = 0.01$ hartree in all calculations.

As a test of the computational method, calculations of $\beta_{ijk}(\omega)$ were performed for the molecules aniline, nitrobenzene and *para*-nitroaniline, which have been the subject of similar calculations by several groups.[22–26] Calculations that included 50 excited states of the molecules in Eq. (1) produced results that were consistent with those of previous studies, in particular, for the signs and magnitudes of the dominant elements of $\beta_{ijk}(\omega)$ for $\hbar\omega = 1.17$ eV. A summary of the results of these calculations has been made available as supplementary material.[27,36]

The right-handed α-helix with stoichiometry $CH_3-(CO-HN-CH_2)_7-H$ had standard torsional angles $\phi = -58°$ and $\psi = -47°$ and *trans* peptide bonds ($\omega = 180°$). The structure was prepared by using HYPERCHEM modeling software,[28] and incorporated standard structures for the glycine residues provided by HYPERCHEM. The α-helix had 3.6 residues per turn, and thus seven glycine residues comprise almost two full turns of the helix. The long axis of the helix (z) was coincident with the inertial axis of a parent α-helical structure that was made up of twenty glycine residues. The model α-helix is shown in Fig. 1(a). Figure 1(b) shows the division of the structure into seven NMA monomers that have the same orientations as the glycine residues. Figure 1(c) is a view down the long axis of the helix in which only the carbonyl groups of the structure are shown. This end-on view shows that each carbonyl group is tilted away from the long axis of the helix.

IV. RESULTS AND DISCUSSION

A. Measurement of nonlinear susceptibilities

A chiral, isotropic surface has full rotational symmetry about the surface normal Z, but lacks mirror planes perpendicular to the surface. The nonlinear susceptibility tensor $\chi_{IJK}^{(2)}$ has four nonzero elements: $IJK = ZZZ, ZXX, XXZ, XYZ$, of which only XYZ is specific to chiral surfaces. The remaining elements are in general nonzero for both chiral and achiral surfaces. It is convenient to express the intensity of second-harmonic radiation in terms of effective susceptibilities f, g, and h, as shown in equation given below, where E_p and E_s are complex amplitudes of incident p- and s-polarized fundamental radiation:[29]

$$I_{2\omega} = |fE_p^2(\omega) + gE_s^2(\omega) + hE_p(\omega)E_s(\omega)|^2. \quad (7)$$

Effective susceptibilities f_p, g_p, and h_p apply for p-polarized second harmonic, and f_s, g_s, and h_s apply for s-polarized second-harmonic radiation. The effective susceptibilities can be measured by observing the variation of second-harmonic intensity with the polarization state of fundamental radiation. Maki *et al.*[29] have given details of this procedure for the case of continuous variation of the polarization state of the fundamental by rotation of a quarter-wave retardation plate. In practice one measures rotation traces $I_{2\omega}(\varphi)$ of the intensity of s- or p-polarized second harmonic as a function of azimuthal angle φ of the quarter-wave retardation plate. The explicit form of $I_{2\omega}(\varphi)$ is given below for the particular case of s-polarized second harmonic, and with the dependence on intensity of fundamental radiation factored out:

$$\begin{aligned} I_{2\omega}(\varphi) = {} & \tfrac{1}{16}[-f_{s1} - 4f_{s2}\cos 2\varphi + f_{s1}\cos 4\varphi \\ & + h_{s1}\sin 4\varphi]^2 + \tfrac{1}{16}[-f_{s2} + 4f_{s1}\cos 2\varphi \\ & + f_{s2}\cos 4\varphi + 2h_{s1}\sin 2\varphi]^2. \end{aligned} \quad (8)$$

In this case the effective susceptibility $g_s = 0$, assuming that only electric dipole interactions are important.[4] In Eq. (8), the second subscripts 1 and 2 refer to real and imaginary parts of the effective susceptibilities, respectively. There are thus three real-valued quantities that fully describe the rotation trace for s-polarized second harmonic: f_{s1}, f_{s2}, and h_{s1}, of which f_{s1} and f_{s2} are nonzero only for chiral surfaces and h_{s1} is in general nonzero for both chiral and achiral surfaces. An attractive feature of this experimental approach is that the chirality of a surface is immediately apparent in the rotation trace $I_{2\omega}(\varphi)$, which is asymmetric about $\theta = 180°$ for chiral surfaces and symmetric for achiral surfaces.

Figure 2 shows rotation traces $I_{2\omega}(\varphi)$ for PBLG and PELG and also for the soluble surfactant dodecylbenzenesulphonic acid (DBSA) adsorbed at the air/water interface. All traces are normalized to a SHG signal that was recorded for a quartz plate in the reference channel. DBSA was selected as an achiral reference for comparison with the chiral polymer films. It can be seen in Fig. 2 that the rotation traces for PBLG and PELG are distinctly asymmetric about $\varphi = 180°$, while the trace for DBSA is symmetric, as expected for chiral and achiral surfaces, respectively. Nonlinear susceptibilities were measured by fitting the rotation traces to Eq. (8), and using the expressions given by Maki, Kauranen, and Persoons to calculate $\chi_{XXZ}^{(2)}$ from h_s and $\chi_{XYZ}^{(2)}$ from f_s. Absolute values were estimated by comparison with separate measurements for a clean air/water interface, for which absolute values of $\chi_{XXZ}^{(2)}$ have been reported.[30,31] The results for PBLG and PELG are summarized in Table I.

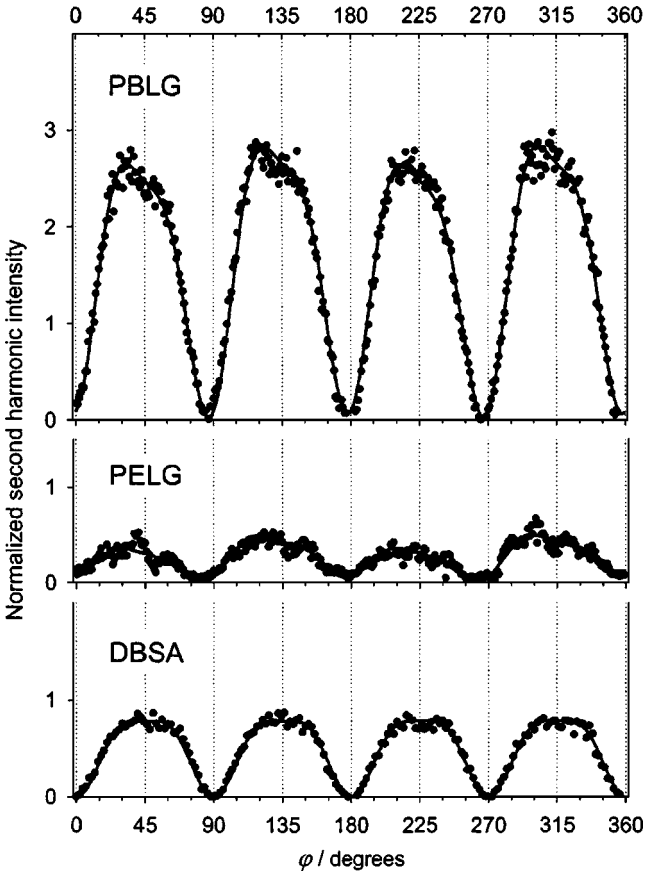

FIG. 2. Rotation traces $I_{2\omega}(\varphi)$ for the polypeptides PBLG and PELG and for the achiral surfactant DBSA adsorbed at the air/water interface. The solid lines are fits of the data to Eq. (8). Note that the traces for the chiral interfaces PBLG and PELG are asymmetric about $\varphi=180°$, and the trace for the achiral interface DBSA is symmetric.

The rotation traces for PBLG and PELG in Fig. 2 were recorded for as-spread films at the air/water interface, with no subsequent compression of the films with the moveable barriers of the trough. From observations of the surface pressure-area isotherms of the polymer films in separate measurements, it was seen that the surface pressure for the SHG measurements was just below the onset of a steep rise in surface pressure. The area per monomer was greater than ~ 21 Å^2. Under these conditions the polymer rods lie parallel to the surface and form solidlike two-dimensional islands which coexist with small residual areas of bare water surface.[9] If the polymer islands are small compared to the area of the incident laser beam (with spot diameter >150 μm) and have random orientations in the surface plane, then the surface is effectively isotropic. A significant departure from in-plane isotropy could introduce a chiral contribution to the SHG response, even in the case where the molecules of the monolayer are achiral.[32] We repeated the measurements of rotation traces on different areas of the surfaces and following rotation of the trough with respect to the surface normal. No indication of anisotropy in the orientational distribution of PBLG or PELG polymer rods was observed. Therefore, the chiral contributions to the rotation traces for PBLG and PELG in Fig. 2 are not attributable to anisotropy of the surfaces, but rather arise from the chirality of the polymer molecules.

TABLE I. Nonlinear susceptibilities of PELG and PBLG monolayer films at the air/water interface, with $\hbar\omega=2.96$ eV. N is the density of monomer constituents in the polmer films. f_s and h_s are effective nonlinear susceptibilities normalized to the susceptibility h_s measured for the clean air/water interface in this work. Two values for $\chi^{(2)}_{XYZ}$ and $\chi^{(2)}_{XXZ}$ shown on separate lines were derived by using alternative values of $\chi^{(2)}_{XXZ}$ for the clean air/water interface as shown in the table. The linear optical properties of the monolayers were assumed to be those of water.

	PELG	PBLG	Air/water interface
$N(\times 10^{18}\ \mathrm{m}^{-2})$	3.2	3.0	⋯
f_s	$0.28+0.14i$	$0.38+0.07i$	⋯
h_s	1.5	4.1	1.0
$\chi^{(2)}_{XYZ}(\times 10^{-22}\ \mathrm{m}^2\ \mathrm{V}^{-1})$	$0.087+0.043i$	$0.12+0.022i$	⋯
	$0.29+0.14i$	$0.39+0.072i$	⋯
$\chi^{(2)}_{XXZ}(\times 10^{-22}\ \mathrm{m}^2\ \mathrm{V}^{-1})$	0.38	1.0	0.25[a]
	1.2	3.4	0.84[b]

[a]Reference 30, $\hbar\omega=2.33$ eV
[b]Reference 31, $\hbar\omega=2.33$ eV.

The results in Table I show that PBLG and PELG monolayers have similar chiral contributions $\chi^{(2)}_{XYZ}$ to the nonlinear susceptibility. The absolute values of $\chi^{(2)}_{XYZ}$ for PBLG and PELG are relatively small, being comparable in magnitude to the achiral susceptibility $\chi^{(2)}_{XXZ}$ of the clean air/water interface. It is interesting to note that the $\chi^{(2)}_{XYZ}$ for PBLG and PELG with $\lambda=417$ nm are similar in magnitude to $\chi^{(2)}_{XYZ}$ for tryptophan derivatives at the air/water interface with $\lambda=564$ nm ($|\chi^{(2)}_{XYZ}|\approx 0.5\times 10^{-22}$ m^2 V^{-1}).[7] These first quantitative measurements of SHG-OA for biomolecules therefore suggest that the effect may generally be rather small.

B. Calculation of nonlinear susceptibilities

In the following we illustrate general features of the nonlinear susceptibility of a monolayer of α-helices by describing computational results for the model α-helix in Fig. 1. We also describe aspects of the microscopic origin of the nonlinear response suggested by the ZINDO/S computational model.

The elements of the macroscopic nonlinear susceptibility tensor $\chi^{(2)}_{IJK}$ were calculated by averaging the molecular tensor β_{ijk} over the orientational distribution of the α-helix.[10] It was assumed that both the twist angle of the helix about its long axis and the orientation of the long axis about the surface normal were randomly distributed, as expected in the experiment. The long axis made a tilt angle θ with the surface normal. In Fig. 3 we show the magnitudes of the effective susceptibilities f_p, g_p, f_s, and h_s calculated from $\chi^{(2)}_{IJK}$ as a function of the tilt angle θ. The fundamental frequency in the calculations was $\hbar\omega=2.96$ eV, which corresponds with the wavelength $\lambda=417$ nm used in the experiment. The plots in Fig. 3 were calculated for an assumed square distribution of the tilt angle about the mean value, with the angular width of the square distribution set to 10°. Closely similar results were obtained for angular widths of 0° and 30°. Note that the achiral susceptibilities f_p, g_p, and h_s go to zero at $\theta=90°$, with the long axis of the helix in the surface plane. A vanishing achiral response is expected for helices lying flat on

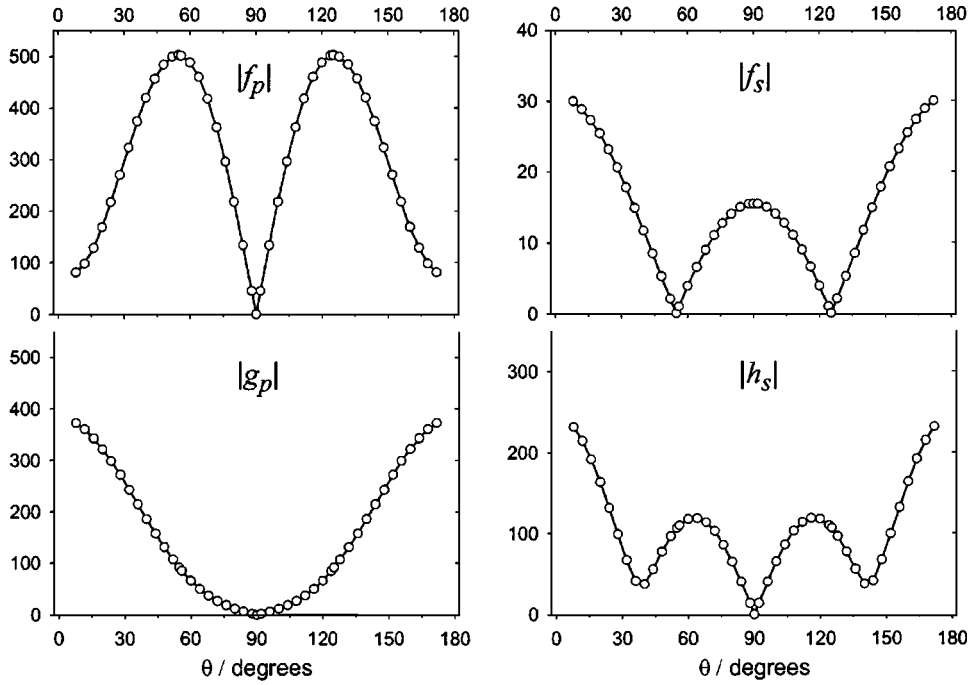

FIG. 3. Calculated nonlinear susceptibilities for the model α-helix, shown as a function of the tilt angle of the long axis of the helix relative to the surface normal. The fundamental frequency was $\hbar\omega = 2.96$ eV. The magnitude of each susceptibility is plotted in the same arbitrary units. Results are shown for an assumed square distribution of the tilt angle about the mean value, with width 10°.

the surface, because in this case there is no polar order in the monolayer. The chiral susceptibility f_s shows a different behavior, being nonzero at $\theta = 90°$ and 0°. The magnitude of the chiral response should vary as $|\cos^2(\theta) - \sin^2(\theta)/2|$, with maxima at $\theta = 0$ and 90° and a vanishing response at $\theta = 54.7°$.[10] From these considerations we should expect that PBLG and PELG monolayers at the air/water interface show a vanishing achiral response and a nonvanishing chiral response. However, we must also consider that a small achiral contribution is expected due to the response of the bare air/water and polymer/water interfaces.

Our results are consistent with the above picture in which an additional achiral component accompanies the chiral response that is intrinsic to the polymer molecules. As shown in Table I, the achiral contribution is significantly larger for PBLG than for PELG. Such an achiral contribution could arise due to asymmetry in the conformations of the ester side chains on the air and water sides of the α-helix. The observation of a more pronounced effect for PBLG may be anticipated from the expected higher nonlinearity of the benzyl-containing side chain of PBLG compared with the ethyl-containing side chain of PELG.

In Fig. 4, calculated achiral $|f_p|$, $|g_p|$, $|h_s|$, and chiral $|f_s|$ susceptibilities are shown as a function of photon energy of the fundamental radiation. The tilt angle was $\theta = 0°$ for the achiral susceptibilities and $\theta = 90°$ for the chiral susceptibility, i.e., the long axis of the model α-helix parallel and perpendicular to the surface normal, respectively. Also shown in Fig. 4 is a calculated (ZINDO/S) absorption spectrum of the model α-helix and an experimental absorption spectrum[33] of poly-(γ-methyl-*L*-glutamate) (PMLG) in trifluoroethanol. The calculated spectrum was produced by broadening all transitions with a Lorentzian line shape with FWHM = 0.43 eV (FWHM—full width at half maximum). There is a close correspondence between the calculated and experimental absorption spectra, which indicates that the ZINDO/S model produced reasonable results for the excitation frequencies of the amide groups of the α-helix. Note that in comparing the model α-helix with PMLG we have ignored the $-COOCH_3$ groups of PMLG. This is reasonable because these groups make a negligible contribution to the UV spectrum of in the region of interest.[33] The absorption spectra in Fig. 4(c) are shown on an energy scale $\hbar\omega/2$, in order to facilitate comparison with the nonlinear susceptibilities. It is clear from this comparison that both the chiral and achiral susceptibilities are resonantly enhanced at the two-photon level, in the region of the amide π-π^* transition of the monomer NMA. The corresponding single-photon excitation energy of NMA is near 6.8 eV (experimental value) (Ref. 19) and the calculated (ZINDO/S) value is 6.6 eV.

C. Achiral contribution to nonlinearity

Experimental measurements have been reported for the sign and magnitude of the vector part of the hyperpolarizability of PBLG dissolved in 1,2-dichloroethane.[34] β_z is the vector component of β_{ijk} on the axis that contains the molecular dipole moment. For an α-helix this is the helical axis *z*. β_z is given in terms of β_{ijk} as shown in equation given below:

$$\beta_z = \beta_{zzz} + \tfrac{1}{3}[\beta_{zxx} + \beta_{zyy} + 2\beta_{xxz} + 2\beta_{yyz}]. \quad (9)$$

Levine and Bethea [34] reported $\beta_z = +2 \times 10^{-31} \pm 50\%$ esu *per monomer* for PBLG for the fundamental frequency $\hbar\omega = 1.17$ eV. Our calculated β_z for the model α-helix composed of seven glycine residues is in excellent agreement with this measurement: $\beta_z(\text{calc}) = +194$ a.u. for $\hbar\omega = 1.17$ eV. This corresponds with +28 a.u. or $+2.4 \times 10^{-31}$ esu per monomer. The positive sign means that β_z has the same sign as the molecular dipole moment.

The ZINDO/S calculations show the origin of the achiral response that underlies β_z. According to the calculations, the

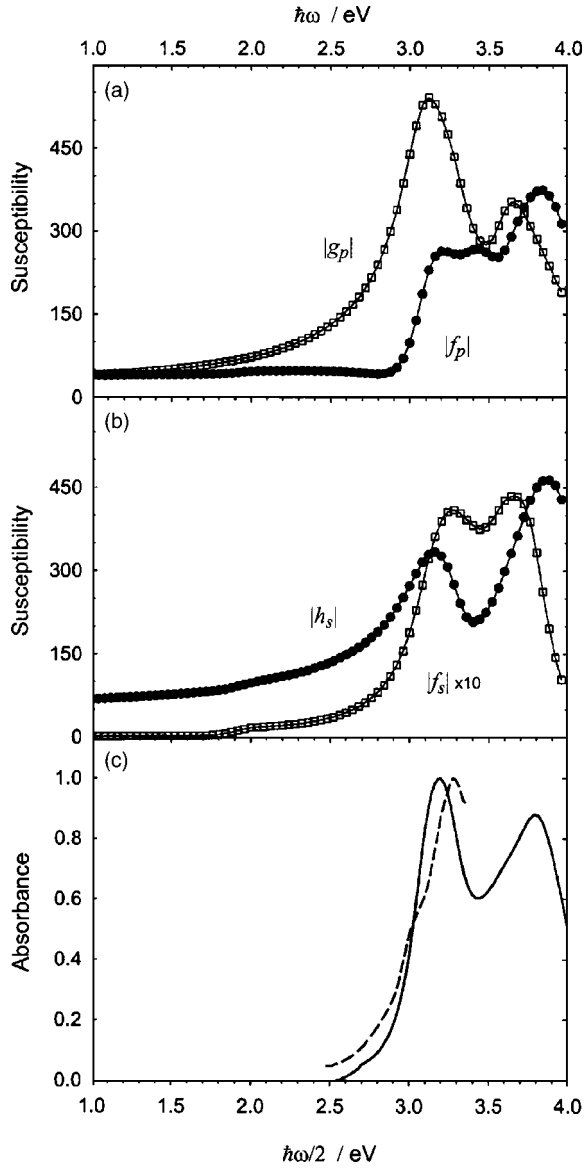

FIG. 4. (a) and (b) Calculated nonlinear susceptibilities for the model α-helix, shown as a function of photon energy of fundamental radiation. The tilt angle of the long axis of the helix relative to the surface normal is 0° for $|g_p|$, $|f_p|$ and $|h_s|$, and 90° for $|f_s|$. The magnitude of each susceptibility is plotted in the same arbitrary units, with $|f_s|$ shown $\times 10$ expanded. (c) Absorption spectrum of polypeptide α-helix. The solid line shows the calculated spectrum and the broken line is an experimental spectrum of poly-(γ-methyl-*L*-glutamate) from Ref. 33 (see the text). Note that the energy scale is $\hbar\omega/2$ in (c) only, to facilitate comparison with the nonlinear susceptibilities.

axial tensor element β_{zzz} is considerably smaller than the other contributing elements in Eq. (9), and furthermore it has the opposite sign. The first and second terms in Eq. (1) give the contributions of off-diagonal, three-state interactions and diagonal, two-state interactions, respectively, to the molecular hyperpolarizability tensor.[11,21] For certain types of chromophores, two-state interactions dominate and a simple interpretation of the nonlinear response can be given. This is the case for push-pull chromophores such as *para*-nitroaniline (PNA), where the two-state contribution is proportional to $(\mu^z_{gn})^2(\mu^z_{nn}-\mu^z_{gg})$, which includes the difference in molecular dipole moments between the ground and excited state. This factor is positive for PNA, which accounts for the positive sign of β_z. However, it is negative for the α-helix, since most of the excited states have much *smaller* dipole moments than the ground state, according to the ZINDO/S calculations. These excited states have substantial charge transfer character associated with transitions between individual amide chromophores of the helix. Thus the two-state contribution to the axial element β_{zzz} is large and negative for the α-helix. In fact all of the tensor elements in Eq. (9) are negative, if only the two-state contributions are considered. However, the three-state contributions are all positive, with the net effect that β_{zzz} is small and negative and all of the other elements in Eq. (9) are positive and relatively large. The ZINDO/S calculations thus indicate that charge transfer transitions of the α-helix have a large influence on the achiral components of the hyperpolarizability tensor.

The computational results in Figs. 3 and 4 show the detailed dependence of the effective susceptibilities on the photon energy of the fundamental light and on the tilt angle θ of the long axis of the helix. A significant feature of the results for $\hbar\omega \approx 3.0$ eV in Fig. 3 is a pronounced dependence of the ratio $|g_p|/|f_p|$ on the tilt angle. The large value of this ratio near $\theta=0$ is a consequence of the relatively low magnitude of β_{zzz}. This ratio is readily measured from experimental $I_{2\omega}(\varphi)$ traces, which could therefore be useful for probing the tilt angle of the helix with respect to the surface normal. The conditions were not suitable for such measurements in the present work because the PBLG and PELG films had $\theta=90°$ and consequently the achiral response of the α-helix was not observed.

D. Chiral contribution to nonlinearity

The chiral response of the model α-helix is much weaker than the achiral response, as shown in Figs. 3 and 4. Furthermore, the chiral susceptibility f_s goes to zero in the limit of zero frequency, which is not the case for the achiral susceptibilities. If the twist angle of the helix about its long axis *z* has a random distribution then the chiral response is proportional to $(\beta_{xyz}-\beta_{yxz})$.[10] The chiral susceptibility therefore vanishes at zero frequency due to Kleinman symmetry, and is nonzero only near resonances.

The absolute values of the chiral susceptibilities for PBLG and PELG in Table I can be compared with the ZINDO/S computed values for the model α-helix. Depending on which value is taken for the susceptibility $|\chi^{(2)}_{XXZ}|_W$ for the clean air/water interface, and with knowledge of the density *N* of peptide monomers present for the PBLG and PELG samples, we find for the chiral susceptibility per monomer unit $|\chi^{(2)}_{XYZ}|/N=(0.30-0.40)\times 10^{-41}$ m^4/V using $|\chi^{(2)}_{XXZ}|_W$ reported by Antoine *et al.*,[30] and $|\chi^{(2)}_{XYZ}|/N=(1.0-1.3)\times 10^{-41}$ m^4/V using $|\chi^{(2)}_{XXZ}|_W$ reported by Rasing *et al.*[31] The range given for each case shows the results for PBLG and PELG. Our calculated value of $|\chi^{(2)}_{XYZ}|/N$ for the α-helix (including a factor of 1/7 to reduce to a per monomer basis) is 4.2 a.u. or 1.5×10^{-41} m^4/V. This value applies for $\hbar\omega \approx 2.96$ eV, which corresponds with the fundamental frequency used in the experiment. Thus, the calculated and experimentally measured chiral susceptibilities are in reasonable agreement, considering that both are subject to a large

uncertainty. The calculation is uncertain because the position of the resonance in $|f_s|$ shown in Fig. 4(b) depends on the details of the computational model, and its amplitude depends on the assumed damping factor Γ included in the calculation of the hyperpolarizability tensor [see Eqs. (1)–(6)].

The chiral contributions to the molecular hyperpolarizability tensor β_{ijk} are those that include x, y, and z in the indices i, j, and k. The computational results showed that the electric dipole transition moments μ_{gn} and $\mu_{n'n}$ for 80 excited states of the α-helix had x, y, and z components almost equally represented. Furthermore, the changes in the static molecular dipole moments of the excited states relative to the ground state $\Delta\mu_n=(\mu_{nn}-\mu_{gg})$ also had significant x, y, and z components, although the z components were dominant. This means that the triple products with $ijk=xyz,yxz,zxy$ in both the first and second terms of Eq. (1) generally have appreciable magnitudes, and the chiral elements β_{xyz}, β_{yxz}, and β_{zxy} are significant. It is apparent that the spatial distributions of the dipole matrix elements that underlie the chiral response depend upon the orientational distribution of the chromophoric subunits of the helix, as illustrated in Fig. 1.

In Fig. 1, the division of the model α-helix into seven NMA monomers is illustrated. The chromophoric subunit is the amide group (–NH–CO–), which has a planar structure with a strong π-π^* transition near 6.6 eV. It is important to note that the plane of each amide group is tilted relative to the helix axis z, such that the CO bond makes an angle $\sim 15°$ with z. The tilt of the CO bond of each amide subunit is illustrated in Fig. 1. This is the situation that pertains for an ideal α-helix with 3.6 residues per turn, as in PBLG and PELG.[35] The tilt of the plane of each amide group relative to the helix axis is significant because it means that each subunit contributes a chiral response, even in the absence of electronic coupling between the chromophores. The essential point is that the axis about which the twist angle ψ of the chromophore is randomly distributed, i.e., the helix axis z does not lie in the plane of the chromophore. In this situation the orientationally averaged ensemble of chromophores is chiral due to asymmetry in the orientational distribution, even when the individual chromophores are planar and hence achiral. This is a particular case of a more general structural effect that Simpson and co-workers[10–12] have recently identified as a possible origin of SHG-OA. This effect is particular for second-order nonlinear optics in that it relies on the partial orientation of molecules, as at an interface, and is not present for isotropic orientational distributions as for molecules in bulk solutions.

If each monomer unit of the polymer can be considered as an independent chromophore, then the overall chiral response is an additive property over the individual chromophores. We found that the main features of the orientationally averaged chiral response $(\beta_{xyz}-\beta_{yxz})$ that was calculated for the α-helix could be reproduced by summing the hyperpolarizabilities of the individual NMA monomer units shown in Fig. 1. Figure 5 shows the frequency dependence of $(\beta_{xyz}-\beta_{yxz})$ as calculated for the model α-helix and for the simplified model of seven independent NMA monomers. The results are similar for the two calculations, particularly near the resonance at $\hbar\omega\approx 3.3$ eV which is associated with the π-π^* transition of NMA. In fact, calculations of $(\beta_{xyz}-\beta_{yxz})$ for each of the seven individual NMA monomers produced the same result, and this was identical to the result in Fig. 5 for the seven independent monomers combined, scaled by a factor of 7. If the orientation of the NMA monomer was adjusted to eliminate the tilt of the plane of the amide chromophore with respect to the z axis, then a much smaller chiral response was calculated. This is expected, because now the plane of the amide group and the axis about which the twist angle is uniformly distributed are coincident, and thus the orientationally averaged ensemble of chromophores is achiral. From this we conclude that the tilt of the plane of each amide group relative to the helical axis of the polymer is the dominant influence on the chiral response of the model α-helix.

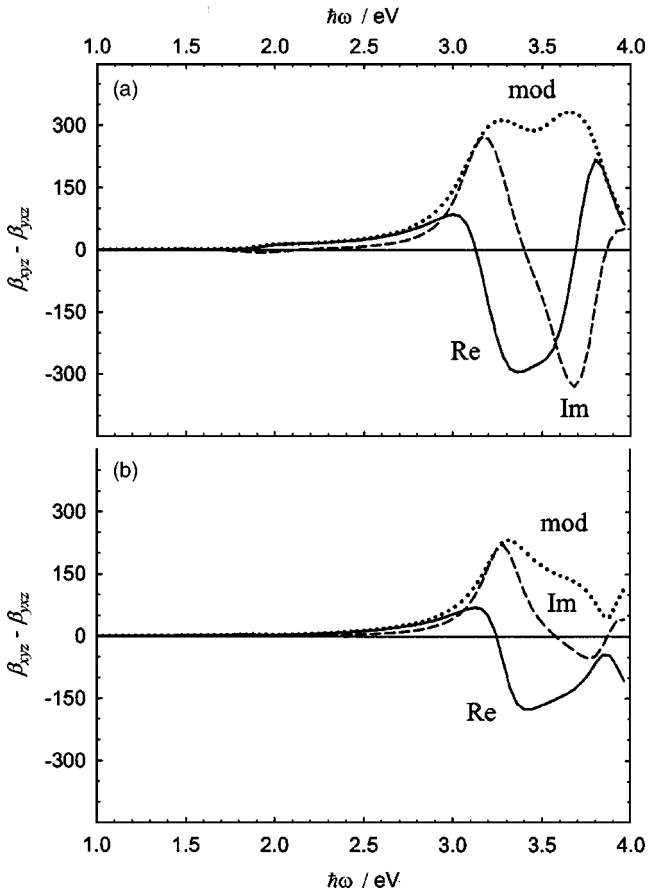

FIG. 5. Calculated difference in hyperpolarizability tensor elements $(\beta_{xyz}-\beta_{yxz})$, shown as a function of photon energy of fundamental radiation for (a) the model α-helix, and (b) the simplified model of seven independent *N*-methylacetamide monomers. The real and imaginary parts and the modulus are plotted in atomic units.

It is easy to see that the tilted NMA monomer discussed above must have nonzero $(\beta_{xyz}-\beta_{yxz})$. For illustration we consider only the influence of the dominant transition $(\pi$-$\pi^*)$ in the low energy region. In this case only a single two-state interaction contributes to the hyperpolarizability, and $(\beta_{xyz}-\beta_{yxz})$ is proportional to $\mu^z_{gn}(\Delta\mu^y_n\mu^x_{gn}-\Delta\mu^x_n\mu^y_{gn})$. Except in the accidental circumstance $\mu^z_{gn}=0$ or $\Delta\mu^y_n\mu^x_{gn}=\Delta\mu^x_n\mu^y_{gn}$, the tilt of the plane of the amide group relative to the helix axis z ensures that μ_{gn} and $\Delta\mu_n$ have nonzero x and y components, and thus $(\beta_{xyz}-\beta_{yxz})$ is nonzero.

We believe that the chiral response of the α-helix observed in our SHG-OA measurements on PBLG and PELG monolayer films is chiefly associated with the structural effect described above. This is suggested by the reasonable agreement between calculated and observed chiral susceptibilities. It should be emphasized that the chiral response is present in a model in which each chromophore is independent with no electronic coupling between the chromophoric subunits. It is possible that such electronic coupling does make a significant contribution to the chiral response through an influence on the matrix elements in Eq. (1), but such an influence would be difficult to isolate from the structural effect. The origin of SHG-OA in a purely structural effect that is present only for partially oriented molecules, as in the case of interfaces, clearly distinguishes SHG-OA from linear optical activity including circular dichroism spectroscopy. The recognition of a structural basis for SHG-OA in this and in previous work will simplify the interpretation of future SHG-OA measurements.

V. CONCLUSION

The microscopic origin of SHG for monolayer films of PELG and PBLG at the air/water interface has been investigated by using a realistic computational model to calculate the molecular hyperpolarizability tensor of a model α-helix. Semiempirical ZINDO/S calculations of the chiral and achiral components of the nonlinear susceptibility are in good agreement with experimental measurements. The achiral response of the model α-helix shows characteristic features that are associated with a relatively low magnitude of the axial tensor element β_{zzz}. This in turn reflects the influence of interamide charge transfer transitions of the α-helix. The computational results indicate that SHG-OA of a polypeptide α-helix is mainly due to a structural effect that is associated with the tilt of the plane of each amide chromophore relative to the long axis of the helix. This structural effect is present in each chromophore, and thus the chiral response is present in a model of independent chromophoric subunits. SHG-OA of a polypeptide α-helix has a structural origin that is directly related to the orientations of the amide subunits of the polymer.

ACKNOWLEDGMENT

The authors thank Dr. Albert Stolow for invaluable technical assistance with the laser source that was used in this study.

[1]S. F. Mason, *Molecular Optical Activity and the Chiral Discriminations* (Cambridge University Press, London, 1982).
[2]S. Sioncke, T. Verbiest, and A. Persoons, Mater. Sci. Eng., R. **42**, 115 (2003), and references cited therein.
[3]P. Fischer, D. S. Wiersma, R. Righini, B. Champagne, and A. D. Buckingham, Phys. Rev. Lett. **85**, 4253 (2000), and references cited therein.
[4]J. J. Maki, M. Kauranen, and A. Persoons, Phys. Rev. B **51**, 1425 (1995).
[5]M. A. Kriech and J. C. Conboy, J. Am. Chem. Soc. **125**, 1148 (2003).
[6]J. C. Conboy and M. A. Kriech, Anal. Chim. Acta **496**, 143 (2003).
[7]S. A. Mitchell and R. A. McAloney, J. Phys. Chem. B **108**, 1020 (2004).
[8]*Circular Dichroism and the Conformational Analysis of Biomolecules*, edited by G. D. Fasman (Plenum, New York, 1996).
[9]M. Fukuto, R. K. Heilmann, P. S. Pershan, S. M. Yu, J. A. Griffiths, and D. A. Tirrell, J. Chem. Phys. **111**, 9761 (1999).
[10]G. J. Simpson, J. M. Perry, and C. L. Ashmore-Good, Phys. Rev. B **66**, 165437 (2002).
[11]G. J. Simpson, J. Chem. Phys. **117**, 3398 (2002).
[12]B. J. Burke, A. J. Moad, M. A. Polizzi, and G. J. Simpson, J. Am. Chem. Soc. **125**, 9111 (2003).
[13]M. J. Frisch, G. W. Trucks, H. B. Schlegel *et al.*, GAUSSIAN 98, Revision A.3 Gaussian, Inc., Pittsburgh, PA, 1998.
[14]J. Ridley and M. Zerner, Theor. Chim. Acta **32**, 111 (1973).
[15]A. D. Bacon and M. C. Zerner, Theor. Chim. Acta **53**, 21 (1979).
[16]J. A. Pople and D. L. Beveridge, *Approximate Molecular Orbital Theory* (McGraw-Hill, New York, 1970).
[17]L. B. Clark, J. Am. Chem. Soc. **117**, 7974 (1995).
[18]R. W. Woody, G. Raabe, and J. Fleischhauer, J. Phys. Chem. B **103**, 8984 (1999).
[19]L. Serrano-Andrés and M. P. Fülscher, J. Am. Chem. Soc. **118**, 12190 (1996).
[20]J. D. Hirst, D. M. Hirst, and C. L. Brooks III, J. Phys. Chem. A **101**, 4821 (1997).
[21]D. Pugh and J. O. Morley, in *Nonlinear Optical Properties of Organic Molecules and Crystals*, edited by D. S. Chemla and J. Zyss (Academic, New York, 1987), Vol. 1, Part II, Chap. 2.
[22]S. J. Lalama and A. F. Garito, Phys. Rev. A **20**, 1179 (1979).
[23]V. J. Docherty, D. Pugh, and J. O. Morley, J. Chem. Soc., Faraday Trans. 2 **81**, 1179 (1985).
[24]S. P. Karna, P. N. Prasad, and M. Dupuis, J. Chem. Phys. **94**, 1171 (1991).
[25]D. Li, T. J. Marks, and M. A. Ratner, J. Phys. Chem. **96**, 4325 (1992).
[26]F. Sim, S. Chin, M. Dupuis, and J. E. Rice, J. Phys. Chem. **97**, 1158 (1993).
[27]See EPAPS Document No. E-JCPSA6-122-710512 for a summary of calculated molecular hyperpolarizabilities of aniline, nitrobenzene and *para*-nitroaniline. A direct link to this document may be found in the online article's HTML reference section. The document may also be reached via the EPAPS homepage (http://www.aip.org/pubservs/epaps.html) or from ftp.aip.org in the directory /epaps/. See the EPAPS homepage for more information.
[28]HYPERCHEM molecular modeling system, release 7.1. Hypercube, Inc., Gainesville, Florida, 2002.
[29]J. J. Maki, M. Kauranen, T. Verbiest, and A. Persoons, Phys. Rev. B **55**, 5021 (1997).
[30]R. Antoine, F. Bianchi, P. F. Brevet, and H. H. Girault, J. Chem. Soc., Faraday Trans. **93**, 3833 (1997).
[31]T. Rasing, G. Berkovic, Y. R. Shen, S. G. Grubb, and M. W. Kim, Chem. Phys. Lett. **130**, 1 (1986).
[32]T. Verbiest, M. Kauranen, and A. Persoons, J. Opt. Soc. Am. B **15**, 451 (1998).
[33]G. Holzwarth and P. Doty, J. Am. Chem. Soc. **87**, 218 (1965).
[34]B. F. Levine and C. G. Bethea, J. Chem. Phys. **65**, 1989 (1976). Note that applicable local field factors were considered to be near unity in this work because of the rodlike shape of PBLG.
[35]H. Block, *Poly(γ-benzyl-L-glutamate) and Other Glutamic Acid Containing Polymers* (Gordon and Breach, New York, 1983).
[36]D. P. Shelton and J. E. Rice, Chem. Rev. (Washington, D.C.) **94**, 3 (1994) (see Ref. 27).